

Observation of $\overline{B}_s^0 \rightarrow J/\psi f'_2(1525)$ in $J/\psi K^+ K^-$ final states

The LHCb Collaboration[†]

Abstract

The decay $\overline{B}_s^0 \rightarrow J/\psi K^+ K^-$ is investigated using 0.16 fb^{-1} of data collected with the LHCb detector using 7 TeV pp collisions. Although the $J/\psi\phi$ channel is well known, final states at higher $K^+ K^-$ masses have not previously been studied. In the $K^+ K^-$ mass spectrum we observe a significant signal in the $f'_2(1525)$ region as well as a non-resonant component. After subtracting the non-resonant component, we find $\mathcal{B}(\overline{B}_s^0 \rightarrow J/\psi f'_2(1525))/\mathcal{B}(\overline{B}_s^0 \rightarrow J/\psi\phi) = (26.4 \pm 2.7 \pm 2.4)\%$.

Keywords: LHC, CP violation, B decays

PACS: 13.25.Hw, 14.40.Nd, 14.40.Be

Submitted to Physical Review Letters

[†]Authors are listed on the following pages.

The LHCb Collaboration

R. Aaij²³, C. Abellan Beteta^{35,n}, B. Adeva³⁶, M. Adinolfi⁴², C. Adrover⁶, A. Affolder⁴⁸,
 Z. Ajaltouni⁵, J. Albrecht³⁷, F. Alessio³⁷, M. Alexander⁴⁷, G. Alkhazov²⁹,
 P. Alvarez Cartelle³⁶, A.A. Alves Jr²², S. Amato², Y. Amhis³⁸, J. Anderson³⁹,
 R.B. Appleby⁵⁰, O. Aquines Gutierrez¹⁰, F. Archilli^{18,37}, L. Arrabito⁵³, A. Artamonov³⁴,
 M. Artuso^{52,37}, E. Aslanides⁶, G. Auriemma^{22,m}, S. Bachmann¹¹, J.J. Back⁴⁴,
 D.S. Bailey⁵⁰, V. Balagura^{30,37}, W. Baldini¹⁶, R.J. Barlow⁵⁰, C. Barschel³⁷, S. Barsuk⁷,
 W. Barter⁴³, A. Bates⁴⁷, C. Bauer¹⁰, Th. Bauer²³, A. Bay³⁸, I. Bediaga¹, S. Belogurov³⁰,
 K. Belous³⁴, I. Belyaev^{30,37}, E. Ben-Haim⁸, M. Benayoun⁸, G. Bencivenni¹⁸, S. Benson⁴⁶,
 J. Benton⁴², R. Bernet³⁹, M.-O. Bettler¹⁷, M. van Beuzekom²³, A. Bien¹¹, S. Bifani¹²,
 T. Bird⁵⁰, A. Bizzeti^{17,h}, P.M. Bjørnstad⁵⁰, T. Blake³⁷, F. Blanc³⁸, C. Blanks⁴⁹,
 J. Blouw¹¹, S. Blusk⁵², A. Bobrov³³, V. Bocci²², A. Bondar³³, N. Bondar²⁹,
 W. Bonivento¹⁵, S. Borghi^{47,50}, A. Borgia⁵², T.J.V. Bowcock⁴⁸, C. Bozzi¹⁶,
 T. Brambach⁹, J. van den Brand²⁴, J. Bressieux³⁸, D. Brett⁵⁰, M. Britsch¹⁰,
 T. Britton⁵², N.H. Brook⁴², H. Brown⁴⁸, A. Büchler-Germann³⁹, I. Burducea²⁸,
 A. Bursche³⁹, J. Buytaert³⁷, S. Cadeddu¹⁵, O. Callot⁷, M. Calvi^{20,j}, M. Calvo Gomez^{35,n},
 A. Camboni³⁵, P. Campana^{18,37}, A. Carbone¹⁴, G. Carboni^{21,k}, R. Cardinale^{19,i,37},
 A. Cardini¹⁵, L. Carson⁴⁹, K. Carvalho Akiba², G. Casse⁴⁸, M. Cattaneo³⁷, Ch. Cauet⁹,
 M. Charles⁵¹, Ph. Charpentier³⁷, N. Chiapolini³⁹, K. Ciba³⁷, X. Cid Vidal³⁶,
 G. Ciezarek⁴⁹, P.E.L. Clarke^{46,37}, M. Clemencic³⁷, H.V. Cliff⁴³, J. Closier³⁷, C. Coca²⁸,
 V. Coco²³, J. Cogan⁶, P. Collins³⁷, A. Comerma-Montells³⁵, F. Constantin²⁸, A. Contu⁵¹,
 A. Cook⁴², M. Coombes⁴², G. Corti³⁷, G.A. Cowan³⁸, R. Currie⁴⁶, C. D'Ambrosio³⁷,
 P. David⁸, P.N.Y. David²³, I. De Bonis⁴, S. De Capua^{21,k}, M. De Cian³⁹, F. De Lorenzi¹²,
 J.M. De Miranda¹, L. De Paula², P. De Simone¹⁸, D. Decamp⁴, M. Deckenhoff⁹,
 H. Degaudenzi^{38,37}, L. Del Buono⁸, C. Deplano¹⁵, D. Derkach^{14,37}, O. Deschamps⁵,
 F. Dettori²⁴, J. Dickens⁴³, H. Dijkstra³⁷, P. Diniz Batista¹, F. Domingo Bonal^{35,n},
 S. Donleavy⁴⁸, F. Dordei¹¹, A. Dosil Suárez³⁶, D. Dossett⁴⁴, A. Dovbnya⁴⁰,
 F. Dupertuis³⁸, R. Dzhelyadin³⁴, A. Dziurda²⁵, S. Easo⁴⁵, U. Egede⁴⁹, V. Egorychev³⁰,
 S. Eidelman³³, D. van Eijk²³, F. Eisele¹¹, S. Eisenhardt⁴⁶, R. Ekelhof⁹, L. Eklund⁴⁷,
 Ch. Elsasser³⁹, D. Elsby⁵⁵, D. Esperante Pereira³⁶, L. Estève⁴³, A. Falabella^{16,14,e},
 E. Fanchini^{20,j}, C. Färber¹¹, G. Fardell⁴⁶, C. Farinelli²³, S. Farry¹², V. Fave³⁸,
 V. Fernandez Albor³⁶, M. Ferro-Luzzi³⁷, S. Filippov³², C. Fitzpatrick⁴⁶, M. Fontana¹⁰,
 F. Fontanelli^{19,i}, R. Forty³⁷, M. Frank³⁷, C. Frei³⁷, M. Frosini^{17,f,37}, S. Furcas²⁰,
 A. Gallas Torreira³⁶, D. Galli^{14,c}, M. Gandelman², P. Gandini⁵¹, Y. Gao³, J-C. Garnier³⁷,
 J. Garofoli⁵², J. Garra Tico⁴³, L. Garrido³⁵, D. Gascon³⁵, C. Gaspar³⁷, N. Gauvin³⁸,
 M. Gersabeck³⁷, T. Gershon^{44,37}, Ph. Ghez⁴, V. Gibson⁴³, V.V. Gligorov³⁷, C. Göbel⁵⁴,
 D. Golubkov³⁰, A. Golutvin^{49,30,37}, A. Gomes², H. Gordon⁵¹, M. Grabalosa Gándara³⁵,
 R. Graciani Diaz³⁵, L.A. Granado Cardoso³⁷, E. Graugés³⁵, G. Graziani¹⁷, A. Greco²⁸,
 E. Greening⁵¹, S. Gregson⁴³, B. Gui⁵², E. Gushchin³², Yu. Guz³⁴, T. Gys³⁷, G. Haefeli³⁸,
 C. Haen³⁷, S.C. Haines⁴³, T. Hampson⁴², S. Hansmann-Menzemer¹¹, R. Harji⁴⁹,
 N. Harnew⁵¹, J. Harrison⁵⁰, P.F. Harrison⁴⁴, T. Hartmann⁵⁶, J. He⁷, V. Heijne²³,
 K. Hennessy⁴⁸, P. Henrard⁵, J.A. Hernando Morata³⁶, E. van Herwijnen³⁷, E. Hicks⁴⁸,
 K. Holubyev¹¹, P. Hopchev⁴, W. Hulsbergen²³, P. Hunt⁵¹, T. Huse⁴⁸, R.S. Huston¹²,

D. Hutchcroft⁴⁸, D. Hynds⁴⁷, V. Iakovenko⁴¹, P. Ilten¹², J. Imong⁴², R. Jacobsson³⁷,
 A. Jaeger¹¹, M. Jahjah Hussein⁵, E. Jans²³, F. Jansen²³, P. Jatou³⁸, B. Jean-Marie⁷,
 F. Jing³, M. John⁵¹, D. Johnson⁵¹, C.R. Jones⁴³, B. Jost³⁷, M. Kaballo⁹, S. Kandybei⁴⁰,
 M. Karacson³⁷, T.M. Karbach⁹, J. Keaveney¹², I.R. Kenyon⁵⁵, U. Kerzel³⁷, T. Ketel²⁴,
 A. Keune³⁸, B. Khanji⁶, Y.M. Kim⁴⁶, M. Knecht³⁸, P. Koppenburg²³, A. Kozlinskiy²³,
 L. Kravchuk³², K. Kreplin¹¹, M. Kreps⁴⁴, G. Krocker¹¹, P. Krokovny¹¹, F. Kruse⁹,
 K. Kruzelecki³⁷, M. Kucharczyk^{20,25,37,j}, T. Kvaratskheliya^{30,37}, V.N. La Thi³⁸,
 D. Lacarrere³⁷, G. Lafferty⁵⁰, A. Lai¹⁵, D. Lambert⁴⁶, R.W. Lambert²⁴, E. Lanciotti³⁷,
 G. Lanfranchi¹⁸, C. Langenbruch¹¹, T. Latham⁴⁴, C. Lazzeroni⁵⁵, R. Le Gac⁶,
 J. van Leerdam²³, J.-P. Lees⁴, R. Lefèvre⁵, A. Leflat^{31,37}, J. Lefrançois⁷, O. Leroy⁶,
 T. Lesiak²⁵, L. Li³, L. Li Gioi⁵, M. Lieng⁹, M. Liles⁴⁸, R. Lindner³⁷, C. Linn¹¹, B. Liu³,
 G. Liu³⁷, J. von Loeben²⁰, J.H. Lopes², E. Lopez Asamar³⁵, N. Lopez-March³⁸,
 H. Lu^{38,3}, J. Luisier³⁸, A. Mac Raighne⁴⁷, F. Machefert⁷, I.V. Machikhiliyan^{4,30},
 F. Maciuc¹⁰, O. Maev^{29,37}, J. Magnin¹, S. Malde⁵¹, R.M.D. Mamunur³⁷, G. Manca^{15,d},
 G. Mancinelli⁶, N. Mangiafave⁴³, U. Marconi¹⁴, R. Märki³⁸, J. Marks¹¹, G. Martellotti²²,
 A. Martens⁸, L. Martin⁵¹, A. Martín Sánchez⁷, D. Martinez Santos³⁷, A. Massafferri¹,
 Z. Mathe¹², C. Matteuzzi²⁰, M. Matveev²⁹, E. Maurice⁶, B. Maynard⁵²,
 A. Mazurov^{16,32,37}, G. McGregor⁵⁰, R. McNulty¹², M. Meissner¹¹, M. Merk²³, J. Merkel⁹,
 R. Messi^{21,k}, S. Miglioranzi³⁷, D.A. Milanese^{13,37}, M.-N. Minard⁴, J. Molina Rodriguez⁵⁴,
 S. Monteil⁵, D. Moran¹², P. Morawski²⁵, R. Mountain⁵², I. Mous²³, F. Muheim⁴⁶,
 K. Müller³⁹, R. Muresan^{28,38}, B. Muryn²⁶, B. Muster³⁸, M. Musy³⁵, J. Mylroie-Smith⁴⁸,
 P. Naik⁴², T. Nakada³⁸, R. Nandakumar⁴⁵, I. Nasteva¹, M. Nedos⁹, M. Needham⁴⁶,
 N. Neufeld³⁷, C. Nguyen-Mau^{38,o}, M. Nicol⁷, V. Niess⁵, N. Nikitin³¹, A. Nomerotski⁵¹,
 A. Novoselov³⁴, A. Oblakowska-Mucha²⁶, V. Obraztsov³⁴, S. Oggero²³, S. Ogilvy⁴⁷,
 O. Okhrimenko⁴¹, R. Oldeman^{15,d}, M. Orlandea²⁸, J.M. Otalora Goicochea², P. Owen⁴⁹,
 B. Pal⁵², J. Palacios³⁹, A. Palano^{13,b}, M. Palutan¹⁸, J. Panman³⁷, A. Papanestis⁴⁵,
 M. Pappagallo⁴⁷, C. Parkes^{50,37}, C.J. Parkinson⁴⁹, G. Passaleva¹⁷, G.D. Patel⁴⁸,
 M. Patel⁴⁹, S.K. Paterson⁴⁹, G.N. Patrick⁴⁵, C. Patrignani^{19,i}, C. Pavel-Nicorescu²⁸,
 A. Pazos Alvarez³⁶, A. Pellegrino²³, G. Penso^{22,l}, M. Pepe Altarelli³⁷, S. Perazzini^{14,c},
 D.L. Perego^{20,j}, E. Perez Trigo³⁶, A. Pérez-Calero Yzquierdo³⁵, P. Perret⁵,
 M. Perrin-Terrin⁶, G. Pessina²⁰, A. Petrella^{16,37}, A. Petrolini^{19,i}, A. Phan⁵²,
 E. Picatoste Olloqui³⁵, B. Pie Valls³⁵, B. Pietrzyk⁴, T. Pilar⁴⁴, D. Pinci²², R. Plackett⁴⁷,
 S. Playfer⁴⁶, M. Plo Casasus³⁶, G. Polok²⁵, A. Poluektov^{44,33}, E. Polcarpo², D. Popov¹⁰,
 B. Popovici²⁸, C. Potterat³⁵, A. Powell⁵¹, J. Prisciandaro³⁸, V. Pugatch⁴¹,
 A. Puig Navarro³⁵, W. Qian⁵², J.H. Rademacker⁴², B. Rakotomiramanana³⁸,
 M.S. Rangel², I. Raniuk⁴⁰, G. Raven²⁴, S. Redford⁵¹, M.M. Reid⁴⁴, A.C. dos Reis¹,
 S. Ricciardi⁴⁵, K. Rinnert⁴⁸, D.A. Roa Romero⁵, P. Robbe⁷, E. Rodrigues^{47,50},
 F. Rodrigues², P. Rodriguez Perez³⁶, G.J. Rogers⁴³, S. Roiser³⁷, V. Romanovsky³⁴,
 M. Rosello^{35,n}, J. Rouvinet³⁸, T. Ruf³⁷, H. Ruiz³⁵, G. Sabatino^{21,k}, J.J. Saborido Silva³⁶,
 N. Sagidova²⁹, P. Sail⁴⁷, B. Saitta^{15,d}, C. Salzmann³⁹, M. Sannino^{19,i}, R. Santacesaria²²,
 C. Santamarina Rios³⁶, R. Santinelli³⁷, E. Santovetti^{21,k}, M. Sapunov⁶, A. Sarti^{18,l},
 C. Satriano^{22,m}, A. Satta²¹, M. Savrie^{16,e}, D. Savrina³⁰, P. Schaack⁴⁹, M. Schiller²⁴,
 S. Schleich⁹, M. Schlupp⁹, M. Schmelling¹⁰, B. Schmidt³⁷, O. Schneider³⁸,

A. Schopper³⁷, M.-H. Schune⁷, R. Schwemmer³⁷, B. Sciascia¹⁸, A. Sciubba^{18,l}, M. Seco³⁶, A. Semennikov³⁰, K. Senderowska²⁶, I. Sepp⁴⁹, N. Serra³⁹, J. Serrano⁶, P. Seyfert¹¹, M. Shapkin³⁴, I. Shapoval^{40,37}, P. Shatalov³⁰, Y. Shcheglov²⁹, T. Shears⁴⁸, L. Shekhtman³³, O. Shevchenko⁴⁰, V. Shevchenko³⁰, A. Shires⁴⁹, R. Silva Coutinho⁴⁴, T. Skwarnicki⁵², A.C. Smith³⁷, N.A. Smith⁴⁸, E. Smith^{51,45}, K. Sobczak⁵, F.J.P. Soler⁴⁷, A. Solomin⁴², F. Soomro¹⁸, B. Souza De Paula², B. Spaan⁹, A. Sparkes⁴⁶, P. Spradlin⁴⁷, F. Stagni³⁷, S. Stahl¹¹, O. Steinkamp³⁹, S. Stoica²⁸, S. Stone^{52,37}, B. Storaci²³, M. Straticiuc²⁸, U. Straumann³⁹, V.K. Subbiah³⁷, S. Swientek⁹, M. Szczekowski²⁷, P. Szczypka³⁸, T. Szumlak²⁶, S. T'Jampens⁴, E. Teodorescu²⁸, F. Teubert³⁷, C. Thomas⁵¹, E. Thomas³⁷, J. van Tilburg¹¹, V. Tisserand⁴, M. Tobin³⁹, S. Topp-Joergensen⁵¹, N. Torr⁵¹, E. Tournefier^{4,49}, M.T. Tran³⁸, A. Tsaregorodtsev⁶, N. Tuning²³, M. Ubeda Garcia³⁷, A. Ukleja²⁷, P. Urquijo⁵², U. Uwer¹¹, V. Vagnoni¹⁴, G. Valenti¹⁴, R. Vazquez Gomez³⁵, P. Vazquez Regueiro³⁶, S. Vecchi¹⁶, J.J. Velthuis⁴², M. Veltri^{17,g}, B. Viaud⁷, I. Videau⁷, X. Vilasis-Cardona^{35,n}, J. Visniakov³⁶, A. Vollhardt³⁹, D. Volyanskyy¹⁰, D. Voong⁴², A. Vorobyev²⁹, H. Voss¹⁰, S. Wandernoth¹¹, J. Wang⁵², D.R. Ward⁴³, N.K. Watson⁵⁵, A.D. Webber⁵⁰, D. Websdale⁴⁹, M. Whitehead⁴⁴, D. Wiedner¹¹, L. Wiggers²³, G. Wilkinson⁵¹, M.P. Williams^{44,45}, M. Williams⁴⁹, F.F. Wilson⁴⁵, J. Wishahi⁹, M. Witek²⁵, W. Witzeling³⁷, S.A. Wotton⁴³, K. Wyllie³⁷, Y. Xie⁴⁶, F. Xing⁵¹, Z. Xing⁵², Z. Yang³, R. Young⁴⁶, O. Yushchenko³⁴, M. Zavertyaev^{10,a}, F. Zhang³, L. Zhang⁵², W.C. Zhang¹², Y. Zhang³, A. Zhelezov¹¹, L. Zhong³, E. Zverev³¹, A. Zvyagin³⁷.

¹ Centro Brasileiro de Pesquisas Físicas (CBPF), Rio de Janeiro, Brazil

² Universidade Federal do Rio de Janeiro (UFRJ), Rio de Janeiro, Brazil

³ Center for High Energy Physics, Tsinghua University, Beijing, China

⁴ LAPP, Université de Savoie, CNRS/IN2P3, Annecy-Le-Vieux, France

⁵ Clermont Université, Université Blaise Pascal, CNRS/IN2P3, LPC, Clermont-Ferrand, France

⁶ CPPM, Aix-Marseille Université, CNRS/IN2P3, Marseille, France

⁷ LAL, Université Paris-Sud, CNRS/IN2P3, Orsay, France

⁸ LPNHE, Université Pierre et Marie Curie, Université Paris Diderot, CNRS/IN2P3, Paris, France

⁹ Fakultät Physik, Technische Universität Dortmund, Dortmund, Germany

¹⁰ Max-Planck-Institut für Kernphysik (MPIK), Heidelberg, Germany

¹¹ Physikalisches Institut, Ruprecht-Karls-Universität Heidelberg, Heidelberg, Germany

¹² School of Physics, University College Dublin, Dublin, Ireland

¹³ Sezione INFN di Bari, Bari, Italy

¹⁴ Sezione INFN di Bologna, Bologna, Italy

¹⁵ Sezione INFN di Cagliari, Cagliari, Italy

¹⁶ Sezione INFN di Ferrara, Ferrara, Italy

¹⁷ Sezione INFN di Firenze, Firenze, Italy

¹⁸ Laboratori Nazionali dell'INFN di Frascati, Frascati, Italy

¹⁹ Sezione INFN di Genova, Genova, Italy

²⁰ Sezione INFN di Milano Bicocca, Milano, Italy

²¹ Sezione INFN di Roma Tor Vergata, Roma, Italy

²² Sezione INFN di Roma La Sapienza, Roma, Italy

²³ Nikhef National Institute for Subatomic Physics, Amsterdam, The Netherlands

²⁴ Nikhef National Institute for Subatomic Physics and Vrije Universiteit, Amsterdam, The Netherlands

²⁵ Henryk Niewodniczanski Institute of Nuclear Physics Polish Academy of Sciences, Kraków, Poland

²⁶ AGH University of Science and Technology, Kraków, Poland

- ²⁷ *Soltan Institute for Nuclear Studies, Warsaw, Poland*
- ²⁸ *Horia Hulubei National Institute of Physics and Nuclear Engineering, Bucharest-Magurele, Romania*
- ²⁹ *Petersburg Nuclear Physics Institute (PNPI), Gatchina, Russia*
- ³⁰ *Institute of Theoretical and Experimental Physics (ITEP), Moscow, Russia*
- ³¹ *Institute of Nuclear Physics, Moscow State University (SINP MSU), Moscow, Russia*
- ³² *Institute for Nuclear Research of the Russian Academy of Sciences (INR RAN), Moscow, Russia*
- ³³ *Budker Institute of Nuclear Physics (SB RAS) and Novosibirsk State University, Novosibirsk, Russia*
- ³⁴ *Institute for High Energy Physics (IHEP), Protvino, Russia*
- ³⁵ *Universitat de Barcelona, Barcelona, Spain*
- ³⁶ *Universidad de Santiago de Compostela, Santiago de Compostela, Spain*
- ³⁷ *European Organization for Nuclear Research (CERN), Geneva, Switzerland*
- ³⁸ *Ecole Polytechnique Fédérale de Lausanne (EPFL), Lausanne, Switzerland*
- ³⁹ *Physik-Institut, Universität Zürich, Zürich, Switzerland*
- ⁴⁰ *NSC Kharkiv Institute of Physics and Technology (NSC KIPT), Kharkiv, Ukraine*
- ⁴¹ *Institute for Nuclear Research of the National Academy of Sciences (KINR), Kyiv, Ukraine*
- ⁴² *H.H. Wills Physics Laboratory, University of Bristol, Bristol, United Kingdom*
- ⁴³ *Cavendish Laboratory, University of Cambridge, Cambridge, United Kingdom*
- ⁴⁴ *Department of Physics, University of Warwick, Coventry, United Kingdom*
- ⁴⁵ *STFC Rutherford Appleton Laboratory, Didcot, United Kingdom*
- ⁴⁶ *School of Physics and Astronomy, University of Edinburgh, Edinburgh, United Kingdom*
- ⁴⁷ *School of Physics and Astronomy, University of Glasgow, Glasgow, United Kingdom*
- ⁴⁸ *Oliver Lodge Laboratory, University of Liverpool, Liverpool, United Kingdom*
- ⁴⁹ *Imperial College London, London, United Kingdom*
- ⁵⁰ *School of Physics and Astronomy, University of Manchester, Manchester, United Kingdom*
- ⁵¹ *Department of Physics, University of Oxford, Oxford, United Kingdom*
- ⁵² *Syracuse University, Syracuse, NY, United States*
- ⁵³ *CC-IN2P3, CNRS/IN2P3, Lyon-Villeurbanne, France, associated member*
- ⁵⁴ *Pontifícia Universidade Católica do Rio de Janeiro (PUC-Rio), Rio de Janeiro, Brazil, associated to ²*
- ⁵⁵ *University of Birmingham, Birmingham, United Kingdom*
- ⁵⁶ *Physikalisches Institut, Universität Rostock, Rostock, Germany, associated to ¹¹*

^a *P.N. Lebedev Physical Institute, Russian Academy of Science (LPI RAS), Moscow, Russia*

^b *Università di Bari, Bari, Italy*

^c *Università di Bologna, Bologna, Italy*

^d *Università di Cagliari, Cagliari, Italy*

^e *Università di Ferrara, Ferrara, Italy*

^f *Università di Firenze, Firenze, Italy*

^g *Università di Urbino, Urbino, Italy*

^h *Università di Modena e Reggio Emilia, Modena, Italy*

ⁱ *Università di Genova, Genova, Italy*

^j *Università di Milano Bicocca, Milano, Italy*

^k *Università di Roma Tor Vergata, Roma, Italy*

^l *Università di Roma La Sapienza, Roma, Italy*

^m *Università della Basilicata, Potenza, Italy*

ⁿ *LIFAELS, La Salle, Universitat Ramon Llull, Barcelona, Spain*

^o *Hanoi University of Science, Hanoi, Viet Nam*

The $\overline{B}_s^0 \rightarrow J/\psi K^+ K^-$ channel has previously been studied only when the $K^+ K^-$ are consistent with the decay of the ϕ meson. This mode has been used to measure the CP violation in \overline{B}_s^0 mixing, ϕ_s , a key probe in the search for physics beyond the Standard Model [1, 2, 3, 4].¹ In addition to the ϕ other resonant or non-resonant final states may appear and affect the CP measurements, including an S-wave contribution [5]. In this paper we study the entire $K^+ K^-$ mass spectrum, including a search for other final states that may be useful in CP violation studies. These states may provide other ways of measuring ϕ_s , in decays with a different spin structure that may be useful for revealing different aspects of CP violation.

We use a 0.16 fb^{-1} data sample collected with the LHCb detector [6] at a center-of-mass energy of 7 TeV. The detector elements most important for this analysis include a vertex locator, a silicon strip device that surrounds the pp interaction region in the LHC, and other downstream tracking devices before and after a 4 Tm dipole magnet. Two ring-imaging Cherenkov detectors are used to identify charged hadrons, while muons are identified using their penetration through iron. This analysis is restricted to events accepted by a di-muon trigger [7]. Subsequent selection criteria are applied that serve to reject background, yet preserve high efficiencies, as determined by Monte Carlo (MC) events generated using PYTHIA [8], and the LHCb detector simulation based on GEANT [9]. To be considered as a $J/\psi \rightarrow \mu^+ \mu^-$ candidate, opposite sign tracks are required to have transverse momentum, p_T , greater than 500 MeV, be identified as muons, and give a good fit to a common vertex.² Di-muon candidates with masses between -48 and $+43$ MeV of the J/ψ peak are selected for further analysis, where the r.m.s. resolution is 13.4 MeV. The invariant mass of the $\mu^+ \mu^-$ pair is constrained to the J/ψ mass for further analysis.

Kaon candidates are selected if their minimum distance from the closest primary vertex is inconsistent with being produced at that vertex. They must be positively identified based on the logarithm of the likelihood ratio comparing two particle hypotheses (DLL). There are two criteria used; loose corresponds to $\text{DLL}(K - \pi) > 0$, while tight has $\text{DLL}(K - \pi) > 10$ and $\text{DLL}(K - p) > -3$. We use the loose criterion for checking kaon identification efficiencies, otherwise the tight criterion is used. In addition, the two kaons must have the sum of the magnitudes of their $p_T > 900$ MeV.

To select \overline{B}_s^0 candidates we require that the $K^+ K^-$ pair and the J/ψ candidate give a good fit to a common secondary vertex with a $\chi^2 < 5$ per degree of freedom. We also require that the \overline{B}_s^0 candidate's decay point must be > 1.5 mm from the primary vertex and that the negative of its momentum vector points back to the primary.

The \overline{B}_s^0 candidate invariant mass is shown in Fig. 1. A clear signal is seen, part of which comes from the previously known $J/\psi \phi$ mode. A check was made for possible resonant states decaying to $J/\psi K^-$ since similar exotic states have been claimed [10], but no obvious structures are visible in the invariant mass spectrum. Figure 2 shows the $K^+ K^-$ invariant mass for both signal and sideband regions, where the signal region

¹Charge conjugate modes are also considered throughout.

²We work in units where $c = 1$.

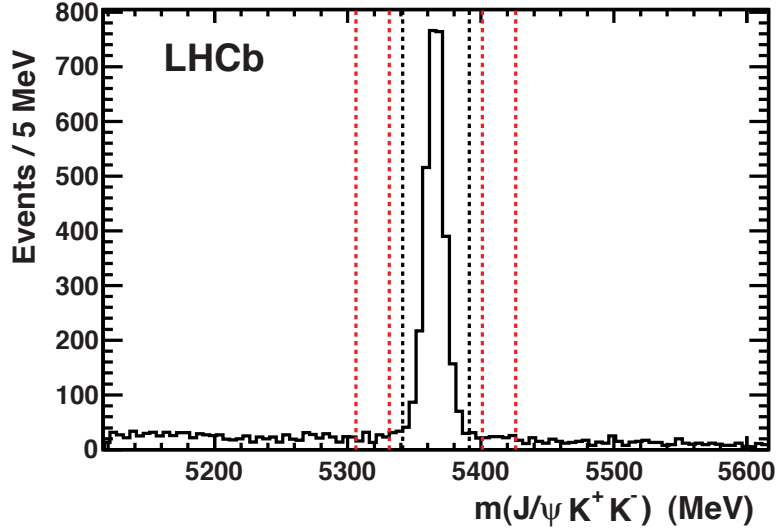


Figure 1: Invariant mass of $J/\psi K^+ K^-$ combinations. The vertical lines indicate the signal and sideband regions.

extends ± 25 MeV around the \bar{B}_s^0 mass peak and the sidebands extend from 35 MeV to 60 MeV on either side of the peak. Apart from the large peak at the ϕ there is a structure

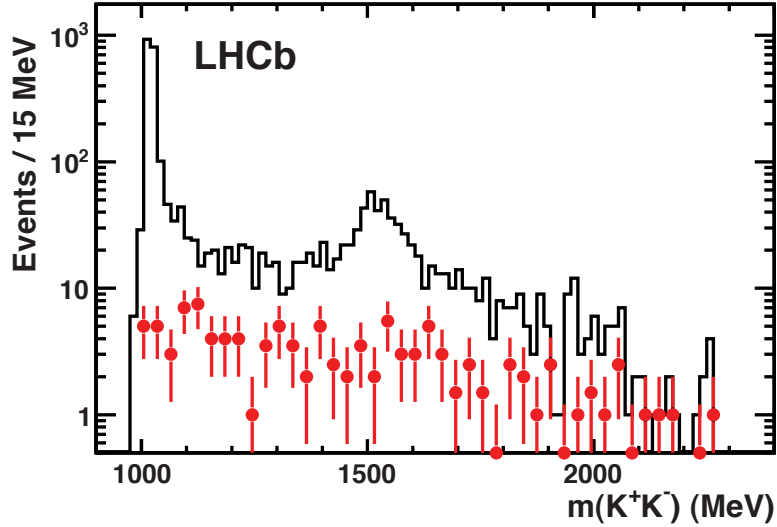


Figure 2: Invariant mass of $K^+ K^-$ combinations. The histogram shows the data in the signal region while the points (red) show the sidebands.

near 1525 MeV. In addition there is an excess of signal events over most of the mass range which we refer to as non-resonant. We investigate the possibility of the peak to be the $f_2'(1525)$ resonance. The PDG quotes the mass of the f_2' state as 1525 ± 5 MeV and the width as 73_{-5}^{+6} MeV [11]. Other states such as the $f_2(1270)$ and the $f_0(1500)$ have small

branching fractions into K^+K^- of less than 5%, and are unlikely to have large rates.

It is possible for the decay $\bar{B}^0 \rightarrow J/\psi K^- \pi^+$ to fake our signal if the π^+ is misidentified as a K^+ . A specific example is given by $\bar{B}^0 \rightarrow J/\psi \bar{K}_2^*(1430)$ decays [12]. To examine if we are sensitive to a reflection of this mode in the 1525 MeV di-kaon mass region, a simulation was performed where the π^+ from the $\bar{K}_2^*(1430)$ was interpreted as a K^+ . Figure 3(a) shows that the reflection of this mode does indeed peak in the di-kaon mass range around 1525 MeV. It also peaks in the \bar{B}_s^0 signal region but is much wider than the \bar{B}_s^0 mass peak. The region 25 – 200 MeV above the \bar{B}_s^0 mass peak provides a sample of misidentified $\bar{B}^0 \rightarrow J/\psi K^- \pi^+$ decays. By measuring the number of \bar{B}^0 candidates in this region we can calculate the number in the \bar{B}_s^0 signal region.

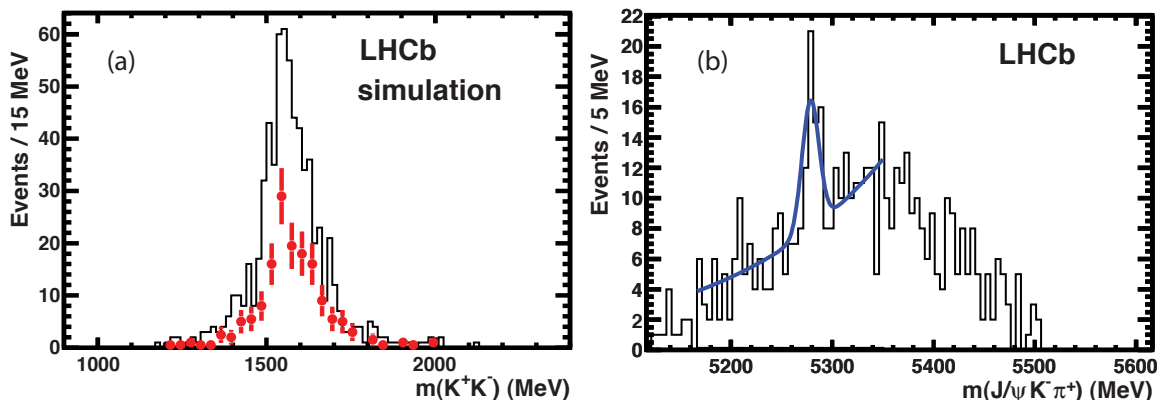


Figure 3: (a) The $m(K^+K^-)$ distribution for simulated $\bar{B}^0 \rightarrow J/\psi \bar{K}_2^*(1430)$ decays where the π^+ from the $\bar{K}_2^*(1430)$ decay is interpreted as a K^+ . The histogram shows $m(K^+K^-)$ in the signal region of \bar{B}_s^0 mass and the points in the sideband region. The simulation corresponds to approximately 8 fb^{-1} of data. (b) The $m(J/\psi K^+ \pi^-)$ distribution for $J/\psi K^+ K^-$ data candidates 25 – 200 MeV above the \bar{B}_s^0 mass, and with $m(K^+K^-)$ within ± 300 MeV of 1525 MeV, reinterpreted as $\bar{B}^0 \rightarrow J/\psi K^- \pi^+$ events. The fit is to a signal Gaussian whose mass and width are allowed to vary as well as a quadratic background.

To determine the size of any \bar{B}^0 reflection in the f_2' mass region we select events where the reconstructed $J/\psi K^+ K^-$ mass is in the range 25 – 200 MeV above the \bar{B}_s^0 mass, reassign each of the two kaons in turn to the pion hypothesis, and plot the $J/\psi K \pi$ mass. The resulting peak at the \bar{B}^0 mass has 36 ± 10 events from the fit shown in Fig. 3(b). We calculate 37 ± 10 events in the \bar{B}_s^0 signal region, using the shape from Monte Carlo simulation, and use this number as a constraint in the fit described below to determine the f_2' parameters and signal yields.

To test the f_2' hypothesis we perform a simultaneous fit to the \bar{B}_s^0 candidate mass and the di-kaon mass. The f_2' signal is parameterized by a spin-2 Breit-Wigner function [13]. The width of the f_2' is fixed to the PDG value of 73 MeV [11]. A contribution from non-resonant K^+K^- is included as a linear function in the di-kaon mass. The contribution

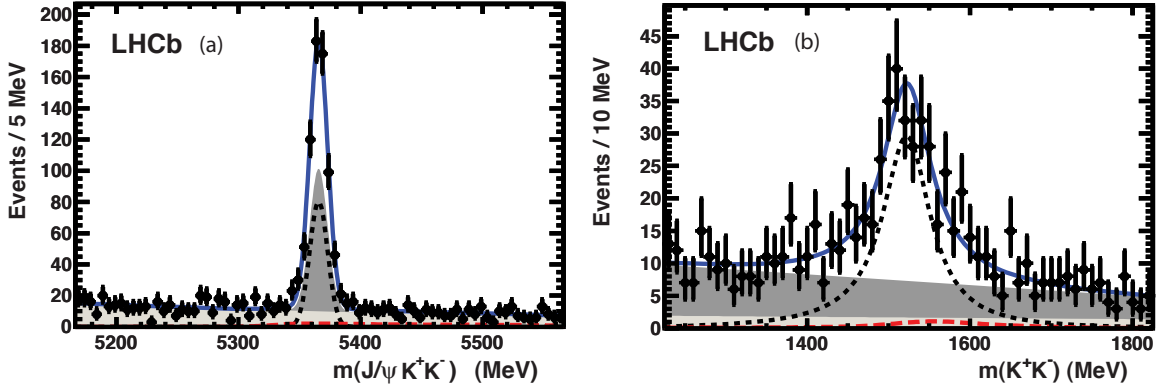


Figure 4: Projections of fits to (a) the \bar{B}_s^0 candidate mass and (b) the di-kaon mass. The f_2' signal is parameterized by a spin-2 Breit-Wigner function whose width is fixed to 73 MeV (dotted curve). The combinatorial background is shown in the light shaded region, while the darker shaded region shows the non-resonant $J/\psi K^+ K^-$ component. The long-dashed (red) line shows the misidentified $\bar{B}^0 \rightarrow J/\psi K^- \pi^+$ decays, and the (blue) line the total.

from the $K^- \pi^+$ reflection is included using the di-kaon and \bar{B}_s^0 mass shapes from the simulation, with the normalization fixed by the event yield in Fig 3(b). The results of the fits are shown in Fig. 4. The f_2' mass from the fit is 1525 ± 4 MeV and the yield is 269 ± 26 events within ± 125 MeV of the mass. If we allow the f_2' width to vary we find a consistent value of 90_{-14}^{+16} MeV. As we have not taken into account possible interferences between the f_2' and other $J/\psi K^+ K^-$ final states we do not provide systematic uncertainties for these values. The decay angle of the J/ψ , $\theta_{J/\psi}$, can test for pure spin-0, or the presence of a higher spin state such as the spin-2 f_2' [11]. Here $\theta_{J/\psi}$ is defined as the angle of the μ^+ with respect to the \bar{B}_s^0 direction in the J/ψ rest frame. It is distributed as

$$f(\cos \theta_{J/\psi}) = (1 - p) \sin^2 \theta_{J/\psi} + \frac{p}{2} (1 + \cos^2 \theta_{J/\psi}), \quad (1)$$

where $1 - p$ is the fraction of helicity zero and p is the fraction of helicity ± 1 . Shown in Fig. 5 is the background subtracted, acceptance corrected $\cos \theta_{J/\psi}$ distribution for $K^+ K^-$ masses in the f_2' region. MC simulation is used to find the acceptance correction. The points are extracted from the joint fit to the $m(J/\psi K^+ K^-)$ and $m(K^+ K^-)$ distributions in the $K^+ K^-$ mass region within 1400 – 1650 MeV for events in the peak above the non-resonant $K^+ K^-$. The fit result is $p = (0.57 \pm 0.13)$, with $\chi^2/\text{number of degrees of freedom}$ (ndof) of 10/8 (27% probability). Fitting only with an S-wave gives χ^2/ndof of 27/9 (0.1% probability), showing that the data are not likely to be pure spin-0, but are compatible with a higher spin state consistent with an f_2' contribution.

The branching fraction of $\bar{B}_s^0 \rightarrow J/\psi f_2'$ relative to $\bar{B}_s^0 \rightarrow J/\psi \phi$ is determined by assuming that the dominant background is S-wave and the signal D-wave, so there is no

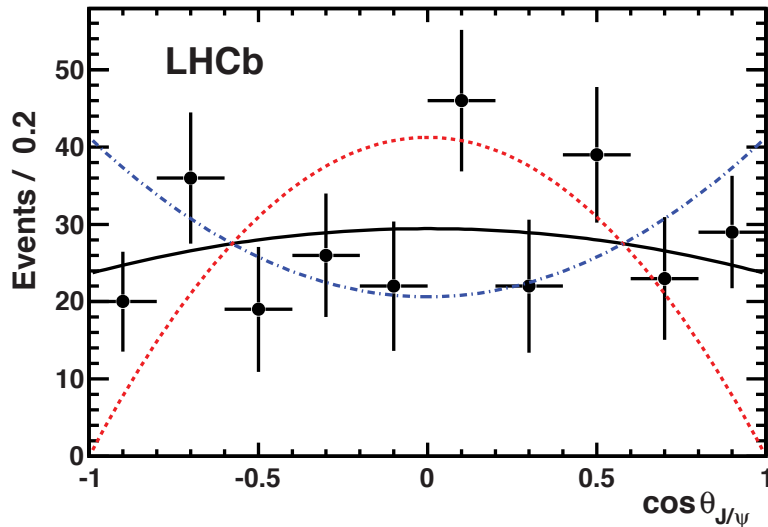


Figure 5: Distribution of $\cos\theta_{J/\psi}$ for $\bar{B}_s^0 \rightarrow J/\psi f_2'$ decays. The background and non-resonant K^+K^- components have been subtracted, and the data have been corrected for acceptance. The fit to Eq. 1 is shown by the solid line. Note that for pure S-wave the distribution would be $\sin^2\theta_{J/\psi}$ ($p = 0$), shown as the dotted curve, while for pure helicity 1 ($p = 1$) the data would be described by the dot-dashed curve.

interference between them.³ The number of $J/\psi K^+K^-$ events is determined by a fit to the \bar{B}_s^0 mass distribution, within ± 20 MeV of the ϕ mass. A small S-wave component in the ϕ mass region of $(4.2 \pm 2.3)\%$ is subtracted [2]. Although there are the same final state particles in both modes, the relative efficiency is $(78 \pm 2)\%$, where the uncertainty arises from simulation statistics. The efficiency ratio differs from unity due to the different p_T distributions of the kaons in the final states. The kaon identification efficiencies are corrected with respect to those given by the MC simulation using a sample of D^{*+} decays, where the kaon can be selected without resorting to PID information. Typical corrections are on the order of 5%.

To find the effective relative rate of f_2' decays we use the fit where the width is allowed to vary. There are 320 ± 33 f_2' events and 1774 ± 42 ϕ events. Correcting for the relative efficiencies and the explicit branching fractions $\mathcal{B}(f_2'(1525) \rightarrow K^+K^-) = (44.4 \pm 1.1)\%$, and $\mathcal{B}(\phi \rightarrow K^+K^-) = (48.9 \pm 0.5)\%$ [11], we measure

$$R \equiv \frac{\mathcal{B}(\bar{B}_s^0 \rightarrow J/\psi f_2'(1525))}{\mathcal{B}(\bar{B}_s^0 \rightarrow J/\psi \phi)} = (26.4 \pm 2.7 \pm 2.4)\%. \quad (2)$$

The systematic uncertainty on R has several contributions, as listed in Table 1. The largest source of uncertainty is f_2' width. The error quoted reflects changing the width

³Although there can be interference as a function of the K^+ decay angle in the f_2' rest frame, integrating over this variable causes the net result to be zero.

by one standard deviation from the fitted value of 90 MeV. The helicity amplitudes of the $J/\psi f'_2$ decay are unknown, unlike the $J/\psi\phi$ amplitudes which are well measured [11]. The difference between the values obtained using helicity zero and helicity one J/ψ MC samples is 4% compared to our central value. The S-wave subtraction of the events in the $J/\psi\phi$ region causes a 2.3% uncertainty. We include an uncertainty for the efficiency as a function of K^+K^- mass, as the tracking could be sensitive to the opening angle of the kaon pair. Modifying the acceptance from a flat to linear function of mass changes the yield by 2.3%. Varying the \bar{B}_s^0 p_T distribution within limits imposed by the data results in a small 0.5% change in the rate. Changing the mass resolution by its error results in a 0.5% change. A PID uncertainty of 1% is added to account for different momentum distributions of the kaons in the two final states. As a check we note that the ratio of the number of events in $J/\psi\phi$ with tight cuts to loose cuts on the kaon identification is $(61\pm 2)\%$ and the simulation gives a consistent $(60\pm 1)\%$. Variation of the background and signal shapes makes small differences.

In conclusion, we have made the first investigation of the $\bar{B}_s^0 \rightarrow J/\psi K^+ K^-$ final state over the entire range of K^+K^- mass. There is a significant non-resonant component that extends under the ϕ region which can affect CP violation measurements [5]. We have also observed $\bar{B}_s^0 \rightarrow J/\psi f'_2(1525)$ decays. The branching fraction ratio relative to $J/\psi\phi$ is

$$\frac{\mathcal{B}(\bar{B}_s^0 \rightarrow J/\psi f'_2(1525))}{\mathcal{B}(\bar{B}_s^0 \rightarrow J/\psi\phi)} = (26.4 \pm 2.7 \pm 2.4)\%, \quad (3)$$

assuming that the background does not interfere with the signal amplitude. This decay mode can also be used to measure CP violation in the \bar{B}_s^0 system, although a different

Table 1: Systematic uncertainties on R .

Source	Change (%)
f'_2 width	6.3
Helicity	4.0
Relative efficiency	2.6
S-wave under ϕ	2.3
K^+K^- mass dependent efficiency	2.3
Background shape	1.3
\bar{B}_s^0 p_T distribution	0.5
\bar{B}_s^0 mass resolution	0.5
PID	1.0
Signal shape	1.0
$\mathcal{B}(f'_2(1525) \rightarrow K^+K^-)$	2.5
$\mathcal{B}(\phi \rightarrow K^+K^-)$	1.0
Total	9.2

transversity analysis than in $J/\psi\phi$ would be required as the final state is a combination of a spin-1 J/ψ and a spin-2 f'_2 state. Some consideration has been given to measuring CP violation in vector-tensor decays [14].

We express our gratitude to our colleagues in the CERN accelerator departments for the excellent performance of the LHC. We thank the technical and administrative staff at CERN and at the LHCb institutes, and acknowledge support from the National Agencies: CAPES, CNPq, FAPERJ and FINEP (Brazil); CERN; NSFC (China); CNRS/IN2P3 (France); BMBF, DFG, HGF and MPG (Germany); SFI (Ireland); INFN (Italy); FOM and NWO (the Netherlands); SCSR (Poland); ANCS (Romania); MinES of Russia and Rosatom (Russia); MICINN, XuntaGal and GENCAT (Spain); SNSF and SER (Switzerland); NAS Ukraine (Ukraine); STFC (United Kingdom); NSF (USA). We also acknowledge the support received from the ERC under FP7 and the Region Auvergne.

References

- [1] LHCb collaboration, R. Aaij et al., *Measurement of the CP violating phase ϕ_s in $\bar{B}_s^0 \rightarrow J/\psi f_0(980)$* , *Phys. Lett.* **B707** (2012) 497–505, [[arXiv:1112.3056](#)].
- [2] LHCb collaboration, R. Aaij et al., *Measurement of the CP-violating phase ϕ_s in the decay $B_s^0 \rightarrow J/\psi\phi$* , [arXiv:1112.3183](#).
- [3] D0 collaboration, V. M. Abazov et al., *Measurement of the CP-violating phase $\phi_s^{J/\psi\phi}$ using the flavor-tagged decay $B_s^0 \rightarrow J/\psi\phi$ in 8 fb⁻¹ of $p\bar{p}$ collisions*, [arXiv:1109.3166](#).
- [4] CDF collaboration, T. Aaltonen et al., *Measurement of the CP-violating phase β_s in $B_s^0 \rightarrow J/\Psi\phi$ decays with the CDF II detector*, [arXiv:1112.1726](#).
- [5] S. Stone and L. Zhang, *S-waves and the measurement of CP violating phases in B_s decays*, *Phys. Rev.* **D79** (2009) 074024, [[arXiv:0812.2832](#)].
- [6] LHCb collaboration, A. Alves Jr. et al., *The LHCb Detector at the LHC*, *JINST* **3** (2008) S08005.
- [7] LHCb collaboration, R. Aaij et al., *Measurement of J/ψ production in pp collisions at $\sqrt{s}=7$ TeV*, *Eur. Phys. J.* **C71** (2011) 1645, [[arXiv:1103.0423](#)].
- [8] T. Sjöstrand, S. Mrenna, and P. Z. Skands, *PYTHIA 6.4 physics and manual*, *JHEP* **0605** (2006) 026, [[arXiv:hep-ph/0603175](#)].
- [9] S. Agostinelli et al., *GEANT4: A simulation toolkit*, *Nucl. Instrum. Meth.* **A506** (2003) 250–303.
- [10] Belle collaboration, R. Mizuk et al., *Dalitz analysis of $B \rightarrow K\pi^+\psi'$ decays and the $Z(4430)^+$* , *Phys. Rev.* **D80** (2009) 031104, [[arXiv:0905.2869](#)].
- [11] Particle Data Group, K. Nakamura et al., *Review of particle physics*, *J. Phys.* **G37** (2010) 075021.
- [12] BaBar collaboration, B. Aubert et al., *Search for the $Z(4430)$ at BaBar*, *Phys. Rev.* **D79** (2009) 112001, [[arXiv:0811.0564](#)].
- [13] Belle collaboration, R. Mizuk et al., *Observation of two resonance-like structures in the $\pi^+\chi_{c1}$ mass distribution in exclusive $\bar{B}^0 \rightarrow K^-\pi^+\chi_{c1}$ decays*, *Phys. Rev.* **D78** (2008) 072004, [[arXiv:0806.4098](#)].
- [14] C. Sharma and R. Sinha, *Angular analysis of B decaying into J/ψ tensor, J/ψ vector and J/ψ scalar modes*, *Phys. Rev.* **D73** (2006) 014016, [[arXiv:hep-ph/0504178](#)].